The analytic conformal compactification of the Schwarzschild spacetime

Jakub Haláček and Tomáš Ledvinka

Faculty of Mathematics and Physics, Institute of Theoretical Physics, Charles University in Prague, V Holešovičkách 2, 180 00 Praha 8, Czech Republic

E-mail: j.halacek@gmail.com and tomas.ledvinka@mff.cuni.cz

Abstract

Among the coordinates used to construct a conformal compactification of the Schwarzschild spacetime, none of them simultaneously extend smoothly both through an event horizon and beyond null infinity. To construct such coordinates, instead of starting with the Kruskal–Szekeres coordinates, we assume direct analytic transformation between Schwarzschild and compactified coordinates and determine their behavior on the event horizon and at null infinity. We then propose an example of such coordinates and illustrate the way they cover the conformally extended Schwarzschild spacetime as well as their suitability for numerical applications.

Keywords: conformal compactification, Schwarzschild spacetime, Penrose–Carter diagrams
PACS numbers: 04.20.−q, 97.60.Lf, 04.25.D−j

1. Introduction

A very useful tool used to discuss various aspects of black-hole spacetimes are the so-called Carter–Penrose diagrams, which are based on the mathematical concept of conformal maps between Lorentzian manifolds. Such maps preserve the causal structure, but they fit the whole spacetime into a finite picture and so they can be useful to illustrate the physical properties of spacetimes such as the structure of horizons or the global shape of worldlines of various observers and null particles, etc.

The standard depiction of compactified Schwarzschild spacetime given in textbooks [1–3] simply shrinks the well-known Kruskal–Szekeres construction of the maximal extension of the Schwarzschild metric into a finite picture. If this depiction appears next to a diagram of the compactified Minkowski spacetime (see figure 1), the two plots seem not only to differ at regions close to the horizon, but also near the null and spatial infinities. This is not supposed to happen as the Schwarzschild spacetime is the most famous member of the family of spacetimes with Minkowski-like infinities—the so-called asymptotically flat spacetimes.
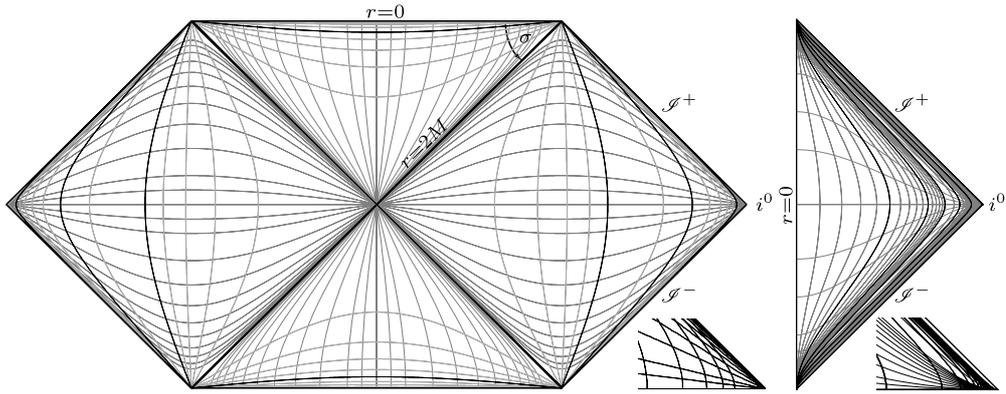
Figure 1. The standard compactified Kruskal diagram of the Schwarzschild spacetime (left) and the Carter–Penrose diagram of the Minkowski spacetime (right). For $M = 1$, a coordinate grid of both corresponds to $r = 0, 0.2, 0.4, \ldots, 3, 4, 5, 6, \ldots, 10, 20, \ldots$ and $|t| = 0, 0.5, 1, 2, \ldots$. The emphasized lines are $r = 0, 1, 2, 3, 5, 10$. The details of regions near i^0 are also displayed.

Since the compactified diagrams of the Schwarzschild black-hole spacetime are regularly used to describe processes from the point-of-view of very distant observers or, e.g., to illustrate geometrical objects stretching to infinity, an important distortion may appear. Typical example can be found in [4], where hyperboloidal slices both in Minkowski and in Schwarzschild spacetimes are studied (see [4], figures 4 and 10). The fact, that curves representing the slices look so differently near the null infinity is only an artifact due to very different behavior of each compactification near infinity. Similarly, also the depiction of the spacelike slicing of the Schwarzschild geometry represented by hypersurfaces $t =$ constant is distorted at infinity (see figure 1). Thus, the standard compactification of the Schwarzschild spacetime cannot, for example, be used to illustrate faithfully the geometry of slices through the spacetime with moving Schwarzschild black hole, because the angle under which slices meet at spatial infinity no longer indicates their relative velocity. Practical problems may also arise when such coordinates are used numerically, since they do not behave well near infinities.

Since both the Schwarzschild geometry and the Carter–Penrose diagrams represent usual textbook topics, several coordinate transformations which should amend this distortion at infinities have been proposed [3, 5]. Even though the existence of analytic coordinates on the manifold conformally-related to the Schwarzschild spacetime that cover both horizon and null infinities has been proven [6]; the available closed-form transformations given in [3, 5] are not analytic in the null infinity. This situation is not limited to the Schwarzschild spacetime—in [7] the dissimilarity of the asymptotic regions between the available Carter–Penrose diagrams for the asymptotically flat exact solutions of Einstein equations and those for the Minkowski spacetime is mentioned be a general feature.

In this paper, we propose coordinates which provide an analytical map on the compactified manifold and thus, lead to the Carter–Penrose diagram of the Schwarzschild spacetime much more similar to the Carter–Penrose diagram of the compactified Minkowski spacetime. In the following, in section 2, we first review the available compactification transformations. Then, in section 3, we show how to make the compactification transformation analytical at null infinity and horizon. In the final section, we discuss the obtained Carter–Penrose diagrams and the implications of the analytic properties of transformations in numerical applications. The well-known properties of the compactification transformation for the Minkowski spacetime, and for asymptotically flat spacetimes in general, are summarized in the appendix.

2. The standard compactification of Kruskal–Szekeres coordinates

The usual compactified diagram of the Schwarzschild spacetime is constructed from the null Kruskal's coordinates using the transformation similar to (A.1) of the Minkowski spacetime. Let us recall, that the radial null geodesic for the Schwarzschild metric

$$\mathrm{d}s^2 = -\left(1 - \frac{2M}{r}\right)\mathrm{d}t^2 + \frac{\mathrm{d}r^2}{1 - \frac{2M}{r}} + r^2\mathrm{d}\omega^2 \tag{1}$$

from which Kruskal's coordinates are derived are given by the partially implicit prescription

$$f(r) = V - U, t = U + V, \theta = \text{constant}, \quad \phi = \text{constant}, \tag{2}$$

where $r_* = f(r)$ is the so-called tortoise coordinate,

$$f(r) = r + 2M \ln\left(\frac{r}{2M} - 1\right). \tag{3}$$

The outgoing radial null geodesics are parametrized by V and labeled by $U, \theta, \phi = \text{constant}$, the ingoing radial null geodesic are parametrized by U.

To achieve the conformal compactification, we need to construct some mapping which will put the infinities $U \to \infty \vee V \to -\infty$ (horizon) and $U \to -\infty \vee V \to +\infty$ (the null infinity) into the inner points of some larger, unphysical manifold. While later, we will show that to obtain an analytical compactification of the Schwarzschild spacetime it is easier to treat at once both the null infinity and the horizon, the standard compactification uses the function $\ln(x)$ to penetrate the horizon first [8] and only then the function $\tan(x)$ is plugged in to fit the Kruskal coordinates into a finite interval [1]. These new coordinates $\mathcal{U}, \mathcal{V} \in (-\pi/2, \pi/2)$ are related to the Schwarzschild coordinates t, r by the transformation

$$f(r(\mathcal{U}, \mathcal{V})) = 2M \ln(\tan \mathcal{V}) + 2M \ln(-\tan \mathcal{U}), \tag{4}$$

$$t(\mathcal{U}, \mathcal{V}) = \Re[2M \ln(\tan \mathcal{V}) - 2M \ln(-\tan \mathcal{U})]. \tag{5}$$

To point out the structure of this transformation, we prefer to use the real part on the right-hand side of (5) instead of the usual $\ln|\tan \mathcal{U}/\tan \mathcal{V}|$. Then,

$$\mathrm{d}s^2 = -\frac{1}{\cos^2 \mathcal{U} \cos^2 \mathcal{V}} \frac{32M^3}{r} \mathrm{e}^{-\frac{r}{2M}} \mathrm{d}\mathcal{U}\,\mathrm{d}\mathcal{V} + r^2\mathrm{d}\omega^2. \tag{6}$$

When $r < 2M$, the transformation (4) becomes a complex-valued implicit function prescription for a real function of the two real variables $r(\mathcal{U}, \mathcal{V})$. Because the metric coefficients in (6) are simple analytic functions of $\mathcal{U}, \mathcal{V}$ and r, the fact that the (here compactified) Kruskal maximal extension can be found is implied by the existence of analytic function $r(\mathcal{U}, \mathcal{V})$ solving (4). Since the Lambert function $W_0(z)$ appearing in the transformation

$$r(\mathcal{U}, \mathcal{V}) = 2M W_0(-e^{-1} \tan \mathcal{U} \tan \mathcal{V}) \tag{7}$$

is analytic on the real axis along the interval $z \in (-e^{-1}, \infty)$ [9], the line element (6) is analytic in the domain, where $-\infty < \tan \mathcal{U} \tan \mathcal{U} < 1$ i.e. $r > 0$, namely at the horizon. The way the Schwarzschild coordinates r, t cover this domain can be seen in figure 1.

It is known that the exponential term $\mathrm{e}^{-r/2M}$ in the Kruskal line element (6) prohibits one to satisfy conditions (A.4) and (A.5) required for asymptotically flat spacetimes. Thus, several coordinate transformations have been given in the literature [3, 5] which should lead to compactification behaving the same way as the Minkowski spacetime for $r \to \infty$. Namely, as the adjective conformal should mean angle-preserving, these coordinates restore the way the curves representing hypersurfaces $t = \text{constant}$ behave near i^0. As an example, let us check the properties of the transformation proposed in [3],

$$\mathscr{U} = \arctan \operatorname{argsinh} \mathcal{U}, \quad \mathscr{V} = \arctan \operatorname{argsinh} \mathcal{V}, \tag{8}$$

which leads to an implicit equation for $r(\mathscr{U}, \mathscr{V})$ given by

$$f(r(\mathscr{U}, \mathscr{V})) = 2M \ln(2 \sinh \tan \mathscr{V}) + 2M \ln(-2 \sinh \tan \mathscr{U}). \tag{9}$$

Using $\Omega_2 = \cos \mathscr{U} \cos \mathscr{V} / (16M^2)$ the conformally related metric reads

$$\widetilde{ds}^2 = -\frac{\coth \tan \mathscr{U} \coth \tan \mathscr{V}}{16M^2} \left(1 - \frac{2M}{r_2}\right) d\mathscr{U} \, d\mathscr{V} + \Omega_2^2 r^2 d\omega^2. \tag{10}$$

With this metric the conformal factor Ω_2 satisfies conditions (A.4) and (A.5), but the metric still cannot be extended through $\mathscr{I}^\pm$ since the function $\coth \tan z$ has an essential singularity at $z = \pm\pi/2$, which simplifies to a discontinuity for real arguments. Similarly the transformation mentioned in [5] which is also based on the Kruskal coordinates provides compactification bounded by $\mathscr{I}$. The fact that the conformally related metric is not available beyond $\mathscr{I}^\pm$ may seem to be only a small issue, but later we will show that this fact can be numerically observed from the behavior of metric coefficients within the physical domain $2M < r < \infty$ (see figure 4).

3. The analytic conformal compactification of the Schwarzschild spacetime

We do not search for the 'right' compactification of the Kruskal coordinates, instead we propose the direct transformation between the Schwarzschild coordinates t, r and the compactified coordinates u, v in the following form:

$$f(r(u, v)) = h(v) + h(-u), \tag{11}$$

$$t(u, v) = h(v) - h(-u). \tag{12}$$

This choice is inspired by the common form of transformations (4) and (9), which is given by the fact that such a transformation changes $-dt^2 + dr_*^2$ into a term proportional to $du \, dv$. The choice of parameters of a yet unknown function h is such that in the exterior Schwarzschild region $r > 2M$ both v and $-u$ are positive. Then, the Schwarzschild line element reads

$$\overline{ds}^2 = -4 \left(1 - \frac{2M}{r}\right) h'(v) \, h'(-u) du \, dv + r^2 d\omega^2. \tag{13}$$

Let us now discuss what kind of function h would lead to an analytic conformal embedding (A.3) of the complete Schwarzschild manifold using the conformal factor $\Omega_3 \sim \cos u \cos v$, which implies, we assign $u = -\pi/2, v = \pi/2$ to the coordinates of null infinities $\mathscr{I}^\pm$ and the horizon $\mathcal{H}^\pm$ is simply put at $u = 0 \vee v = 0$. The transformation (11) again represents a complex-valued implicit equation for the real function $r(u, v)$. To prescribe precisely the behavior of the transformation function $h(x)$ in the complex domain, we decompose it into

$$h(x) = \alpha(x) + 2M \ln \beta(x), \tag{14}$$

where α, β are the analytic functions on $(-\pi, \pi)$ up to simple poles at $\pm\pi/2$ (i.e. at $\mathscr{I}^\pm$, see equation (19)). Indeed, α and β are also restricted by the fact that for a regular transformation $h'(x) \neq 0$ on this interval.

From (3), we see that β should become negative for $r < 2M$ so that imaginary parts on both sides of (11) match due to the common factor $2M$ in front of the logarithm in (14) and (3). The solution of (11) can be given using the Lambert function

$$r = 2M \left[1 + W_0 \left(\beta(v)\beta(-u) \, e^{\frac{\alpha(v)+\alpha(-u)}{2M}-1}\right)\right], \tag{15}$$

which (using $W_0(x) \sim x$) implies that the analytic covering of the horizon requires

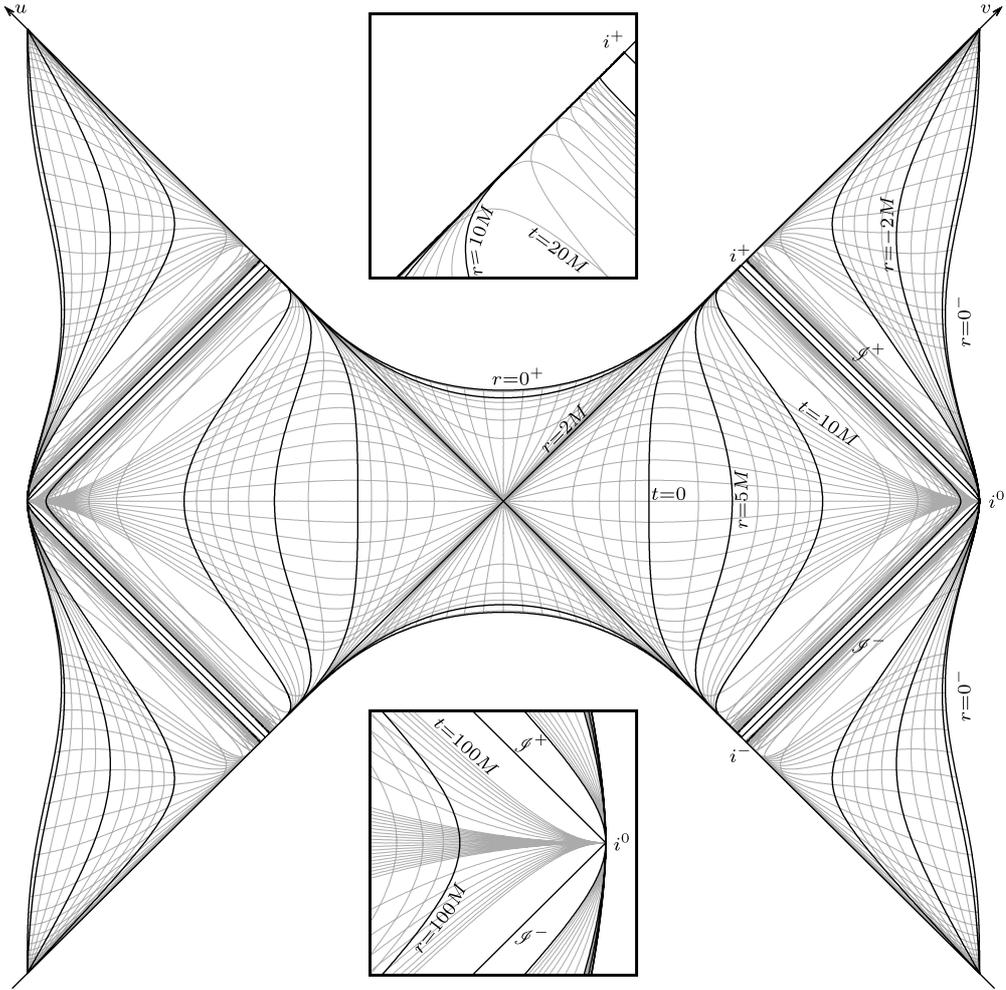$$\alpha(x) \sim 1, \beta(x) \sim x \text{ for } x \simeq 0. \tag{16}$$

Figure 2. The Carter–Penrose diagram of the Schwarzschild spacetime and its analytic extension beyond $\mathscr{I}^{\pm}$ using coordinates (21). A compactification scale $\mu = 3M$ is used. A coordinate grid corresponds to $r/M = 0, 0.5, 1, 1.2, \ldots, 2.8, 3, 4, 5, 6, \ldots, 10, 20, \ldots, 100, \infty, -100, -90, \ldots, -10, -9, \ldots, -1, 0$ and $|t/M| = 0, 1, \ldots, 10, 20, \ldots, 100$. The emphasized lines are $|r/M| = 0, 1, 2, 3, 5, 10, 100$.

We have to further restrict α, β so that the conformally related metric $\widetilde{g}$ (primarily its metric component $\widetilde{g}_{\theta\theta}$) is analytic near $\mathscr{I}^{\pm}$. Equation (15) cannot be used directly as we would need to regularize expression $0.W(\infty e^{\infty})$. We rather decompose $\sqrt{\widetilde{g}_{\theta\theta}} = r\Omega$ into a sum of two terms

$$r\Omega = [\alpha(v) + \alpha(-u)]\,\Omega + [r - \alpha(v) - \alpha(-u)]\,\Omega \tag{17}$$

and then we require both of them to be the analytic functions. This for the first term simply yields $\alpha(v) \sim 1/\Omega$ near $\mathscr{I}^{+}$ and $\alpha(-u) \sim 1/\Omega$ near $\mathscr{I}^{-}$. The analytic properties of the second term on the right-hand side of (17) are for an analytic conformal factor Ω equivalent to the properties of an auxiliary function $\psi(u, v)$, we define by the following relation:

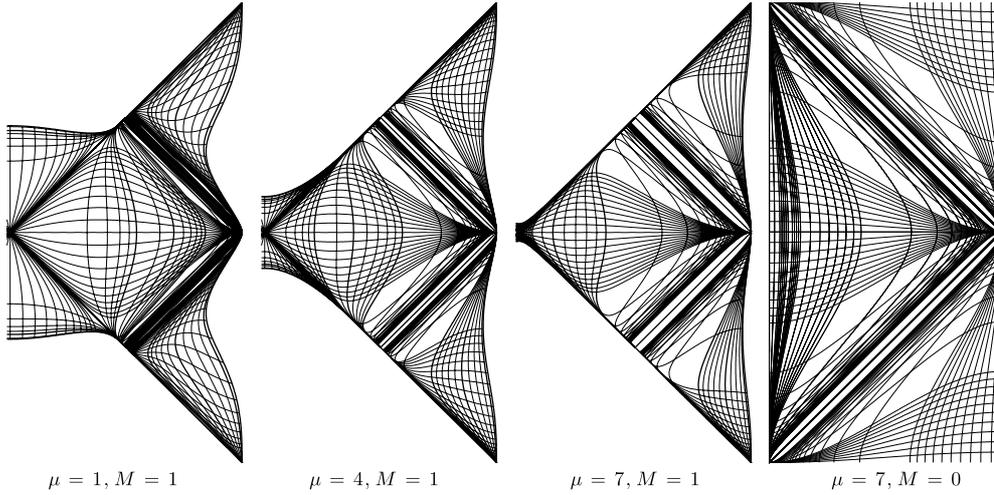$$2M[1 + \psi(u, v)] \equiv r - \alpha(v) - \alpha(-u) = 2M \ln \frac{\beta(v)\beta(-u)}{\frac{r}{2M} - 1}. \tag{18}$$

$\mu = 1, M = 1$ $\mu = 4, M = 1$ $\mu = 7, M = 1$ $\mu = 7, M = 0$

Figure 3. The Carter–Penrose diagram of the Schwarzschild spacetime with three different choices of the compactification scale μ. A compactified Minkowski spacetime is shown on the right panel. To construct this diagram, the transformation (A.1) is plotted with the factor 2, therefore, replaced by $1/\mu$ so that $\mu = 7$ can be used to make the outer regions of the two right panels match.

We can rewrite this definition as an implicit equation

$$\psi(u, v) = -1 - \ln \frac{\frac{1}{\alpha(-u)} + \frac{1}{\alpha(v)} + 2M \frac{1}{\alpha(-u)} \frac{1}{\alpha(v)} \psi(u, v)}{2M \frac{\beta(-u)}{\alpha(-u)} \frac{\beta(v)}{\alpha(v)}}. \tag{19}$$

If we consider e.g. $\mathscr{I}^+$, where $1/\alpha(v) \to 0$ as $v \to \pi/2$, the right-hand side of (19) does not depend on ψ there and (19) thus, explicitly determines the values of $\psi(u, v = \pi/2)$. Indeed, we also need that the ratio $\beta(v)/\alpha(v) \sim 1$ for $v \to \pi/2$, i.e. the poles of both functions must cancel out:

$$\alpha(x) \sim \beta(x) \sim \frac{1}{\cos x} \text{ for } x \simeq \frac{\pi}{2}. \tag{20}$$

With this behavior of α and β at $\mathscr{I}^\pm$, both sides of (19) are guaranteed to have different derivatives with respect to ψ and the implicit function theorem then implies that ψ is an analytic function at $\mathscr{I}^\pm$. No further restrictions on α and β are implied by a regularity of the metric component $\widetilde{g}_{uv}$.

We found a reasonably simple choice of function

$$h(x) = \frac{\mu}{\cos x} + 2M \ln \frac{\tan x}{1 + \cos x} \tag{21}$$

and of the conformal factor

$$\Omega(u, v) = \frac{\cos u \cos v}{4\mu^2}, \tag{22}$$

which together satisfy all necessary conditions if the compactification scale $\mu > 0.38896697\ldots M$ (this bound comes from $h' \neq 0$). The Carter–Penrose diagram with a grid of Schwarzschild coordinates plotted for $\mu = 3M$ is shown in figure 2. As a consequence of the analytic properties of the transformation we can see in this figure also the regions behind $\mathscr{I}^\pm$. We suppose that in some applications the conformal geometry in a small region behind $\mathscr{I}^\pm$ may be exploited, e.g. if numerical methods require grid points there. The full extension
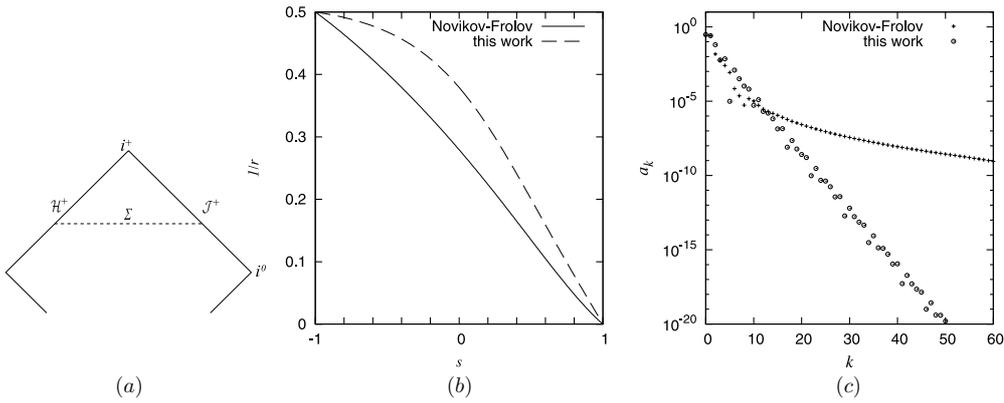
Figure 4. A comparison of the analytic coordinates (11) with (21) and coordinates suggested in [3]. (*a*) An illustration of the hypersurface connecting horizon and null infinity. (*b*) A plot of function $1/r(\mathscr{U}(s), \mathscr{V}(s))$ and $1/r(u(s), v(s))$ (see equations (9) and (11)) on a linear combination of either coordinates which represents radial parameter within the hypersurface. (*c*) The coefficients of the Chebyshev expansion of functions $1/r(\mathscr{U}(s), \mathscr{V}(s))$ and $1/r(u(s), v(s))$. One can see, that the coefficients of $1/r(u(s), v(s))$ decay much faster. See discussion in the text for an example of practical implications.

up to the $r \to 0^-$ available in figures 2 and 3 does not necessarily have practical applications, but it enables a direct visual comparison with the well-known conformal embedding of the Minkowski spacetime into Einstein static universe. In figure 3, for larger compactification scales μ the interior region ($r < 2M$) of the black hole on the diagram shrinks, but the regions near i^0 (both the physical one and those beyond $\mathscr{I}^\pm$) resemble more and more the compactified Minkowski spacetime (see, e.g, the behavior of slices $t =$ constant near i^0).

Another common feature—worldline $r = 0^-$ touching the physical region 'from behind' $\mathscr{I}$ at i^0—illustrates the fact, that (logarithmic) singularity is present at i^0, when $M > 0$ (see, e.g., [10, 11] for its detailed description).

4. Concluding remarks

The main visual difference between the compactified diagrams of the Schwarzschild black hole spacetime of figures 1 and 2 is, indeed, the angle σ at which the singularity $r = 0$ approaches $i^\pm$. In both cases, the coordinate transformations have the form of equation (11) so the angle σ is given by the ratio of derivatives $h'(0)/h'(\pi/2)$. The straight shape of the singularity $r = 0$ in figure 1 is thus, related to the very symmetric form of the transformation function $h_{\mathrm{MTW}}(x) = 2M \ln \tan(x)$ (this substitution turns (11) into (4)) for which $h_{\mathrm{MTW}}(\pi/2 - x) = -h_{\mathrm{MTW}}(x)$. On the other hand, the conditions (16) and (20) for the analytic extension of coordinates through $\mathscr{I}^\pm$ and $\mathscr{H}^\pm$ are different and no similar relation applies.

If we take coordinate (8) as proposed in [3], the Carter–Penrose diagram would in the physical regions look very similar to the analytic one in figure 2. But as we already mentioned this transformation does not yield an analytic coverage of null infinity. Even though the analytic properties of transformations cannot be easily seen from a plot, they may still have practical implications. As an example, let us consider a situation, where we would like to solve numerically a problem involving an object which spans from horizon $\mathscr{H}^+$ to null

infinity $\mathscr{I}^+$, e.g., the hyperboloidal hypersurfaces discussed in [12]. Assume also, that the problem can be cast into the form of a differential equation. The coefficients of this differential equation would contain the Schwarzschild geometry represented by function $1/r$ depending on the compactified coordinates and the regularity of these coefficients would determine the regularity of the solution and, e.g., the behavior of the numerical methods used to find this solution. Since various choices of the compactified coordinates yield significant differences in the coordinate dependence of $1/r$, as will be illustrated below, we can observe differences between the compactified coordinates even for problems formulated completely inside the physical spacetime $r < \infty$.

In figure 4, the analytic coordinates (11) with (21) and the coordinates suggested in [3] are compared. First, we show a plot of function $1/r(s)$ when parameter s linearly advances along a straight line from horizon to null infinity either in compactified coordinates $\mathscr{U}, \mathscr{V}$ or u, v (as illustrated in figure 4(a)). Indeed, one cannot distinguish on this plot which of the functions behaves better. To test this, both functions are decomposed into the Chebyshev series $1/r(s) = \sum a_k T_k(s)$ and the absolute values of the coefficients a_k are plotted as a function of k in figure 4(c). One can see that for analytic compactification, the coefficients decay much faster (exponentially). This indicates some of the practical implications of using analytic Carter–Penrose compactifications: numerical methods which require (or take advantage of) the good analytic properties of the function involved would provide better (or faster) results.

Acknowledgments

Appendix. Asymptotically flat spacetimes

The standard way to introduce the notion of asymptotically flat spacetimes refers to the Minkowski spacetime. Therefore, the coordinates $\bar{u}_M, \bar{v}_M$ are usually given by the transformation

$$2r_M = \tan \bar{v}_M - \tan \bar{u}_M, \quad 2t_M = \tan \bar{v}_M + \tan \bar{u}_M, \tag{A.1}$$

which changes the usual Minkowski line element in spherical coordinates $ds_M^2 = -dt_M^2 + dr_M^2 + r_M^2 \, d\omega^2$ with $d\omega^2 = d\theta^2 + \sin^2 \theta d\phi^2$ into

$$\overline{ds}_M^2 = \frac{1}{\cos^2 \bar{u}_M \cos^2 \bar{v}_M} \left(-d\bar{u}_M d\bar{v}_M + \frac{1}{4} \sin^2 (\bar{v}_M - \bar{u}_M) \, d\omega^2 \right). \tag{A.2}$$

The infinities of the Minkowski spacetime M appear on the boundary $\mathscr{I} : \bar{u}_M = -\pi/2 \vee \bar{v}_M = \pi/2$, and depending upon the character of geodesics which end at those points, the spacelike infinity (i^0), the future and past null infinity ($\mathscr{I}^\pm$), and the future and past time-like infinity ($i^\pm$) can be distinguished. Then, using the conformal factor $\Omega_M = \cos \bar{u}_M \cos \bar{v}_M$ which can be clearly identified in (A.2), we obtain a larger manifold $\widetilde{M}$ with metric $\widetilde{ds}_M^2 = \Omega_M^2 \overline{ds}_M^2$ regular on $\mathscr{I}$. The coordinates $\widetilde{u}_M = \bar{u}_M, \widetilde{v}_M = \bar{v}_M$ are no longer restricted to $[-\pi/2, \pi/2] \times [-\pi/2, \pi/2]$.

The choice of the compactified coordinates and the conformal factor above are restricted by the requirements present in the definition of the class of the *asymptotically flat spacetimes* [2, 13, 14]: the coordinates and the conformal factor Ω must lead to the conformally related metric

$$\widetilde{ds}^2 = \Omega^2 ds^2 \tag{A.3}$$

regular at null infinity and the conformal factor must vanish at infinity with the leading terms in its power expansion near $\mathscr{I}$ being

$$\Omega(\mathscr{I}^{\pm}) = 0, \quad \widetilde{\nabla}_{\mu}\Omega(\mathscr{I}^{\pm}) \neq 0, \tag{A.4}$$

$$\Omega(i^0) = 0, \widetilde{\nabla}_{\mu}\Omega(i^0) = 0, \quad \widetilde{\nabla}_{\mu}\widetilde{\nabla}_{\nu}\Omega(i^0) = 2\widetilde{g}_{\mu\nu}(i^0). \tag{A.5}$$

Note that a simple choice of the conformal factor $\Omega = 1/r$ does not satisfy (A.5) despite the fact that such a choice is sometimes suggested.

References

[1] Misner Ch W, Thorne K S and Wheeler J A 1973 *Gravitation* (San Francisco: Freeman)

[2] Wald R M 1984 *General Relativity* (Chicago, IL: University of Chicago Press)

[3] Frolov V and Novikov I 1998 *Black Hole Physics: Basic Concepts and New Developments (Fundamental Theories of Physics)* (Berlin: Springer)

[4] Zenginoğlu A 2008 Hyperboloidal foliations and scri-fixing *Class. Quantum Grav.* **25** 145002

[5] Grøn Ø and Hervik S 2007 *Einstein's General Theory of Relativity: With Modern Applications in Cosmology* (Berlin: Springer)

[6] Friedrich H 2003 Conformal geodesics on vacuum space-times *Commun. Math. Phys.* **235** 513–43

[7] Griffiths J B and Podolský J 2009 *Exact Space-Times in Einstein's General Relativity* (Cambridge: Cambridge University Press)

[8] Kruskal M D 1960 Maximal extension of Schwarzschild metric *Phys. Rev.* **119** 1743–5

[9] Corless R M, Gonnet G H, Hare D E G, Jeffrey D J and Knuth D E 1996 On the Lambert W function *Adv. Comput. Math.* **5** 329

[10] Schmidt B G and Stewart J M 1979 The scalar wave equation in a schwarzschild space-time *Proc. R. Soc.* A **367** 503–25

[11] Herberthson M 1999 On the differentiability conditions at spacelike infinity *Class. Quantum Grav.* **15** 3873

[12] Ohme F, Hannam M, Husa S and Murchadha N Ó 2009 Stationary hyperboloidal slicings with evolved gauge conditions *Class. Quantum Grav.* **26** 175014

[13] Ashtekar A and Hansen R O 1978 A unified treatment of null and spatial infinity in general relativity: I. Universal structure, asymptotic symmetries, and conserved quantities at spatial infinity *J. Math. Phys.* **19** 1542–66

[14] Penrose R 1964 Gravitational radiation *Relativity, Groups and Topology* ed C M DeWitt and B DeWitt (New York: Gordon and Breach) pp 563–84